Indonesian Journal of Science & Technology

Journal homepage: http://ejournal.upi.edu/index.php/ijost/

Module-Scale Simulation of Forward Osmosis Module-Part A: Plate-and-Frame

Muhammad Roil Bilad

Department of Chemical Engineering, Universiti Teknologi Petronas, Bandar Seri Iskandar, Perak 32610, Malaysia

*Corresponding author: Email: mroil.bilad@utp.edu.my; Tel.: +605368 7579

A B S T R A C T

In forward osmosis (FO), a semi-permeable membrane separates a concentrated draw and a diluted feed solution. FO has emerges as a promising alternative for various applications. To support further development of FO process, a larger scale optimization is required to accurately envisage the most critical factors to be explored. In this study, we applied a mass-transfer model coupled with the mass conservation and area discretization to simulate the performance of plate-and-frame FO modules (10 sheets of 1x1m). Effects of numerous parameters were simulated: modes, flow orientations (co-, counter- and cross-currents), spacers and spacer properties, membrane parameters and operational parameters. Results show that counter-current flow orientation offers the highest flux with minimum spatial distribution. Module performance can be improved by developing FO membrane through reducing membrane structural (S) parameter and increasing water permeability (A): increasing A-value only significant at low S-value, and vice versa (i.e., for A-value of 1 LMH/atm, S-value must be below 50 µm). Furthermore, inclusion of spacer in the flow channel slightly increases the flux (merely up to 2%). Module performance can also be enhanced by increasing feed flow rate, lowering solute in the feed and increasing solute in the draw solution.

A R T I C L E I N F O

Article History:
Submitted/ Received 09 Jun 2016
First Revised 23 Jul 2016
Accepted 14 Aug 2016
First Available online 19 Aug 2016
Publication Date 01 Sep 2016

Keyword:
Forward osmosis,
Module design,
Plate-and frame module,
Concentration polarization,
Dilution and concentration effect.

1. INTRODUCTION

In forward osmosis (FO), a semi-permeable membrane separates a concentrated (draw) and a diluted (feed) solution. The osmotic pressure difference between both solutions drives the permeation of water across the membrane from the feed to the draw side. A selectively permeable membrane allows passage of water, but largely rejects solute molecules and ions. (Bilad *et al.*, 2016)

FO has emerges as a promising alternative for various applications because of its several key advantages. FO membrane fouling propensity is considered low and more reversible (Achilli *et al.,* 2009; S. Lee *et al.,* 2010; Mi & Elimelech, 2010). FO process also basically does not require hydraulic pressure (only for pumping/circulation, and by discounting the necessary of draw solution recovery). FO also offers compelling solution for concentrating of various recalcitrants (emerging contaminants, pharmaceuticals, etc) in wastewater that often bypass all treatment processes and eventually accumulate and untreated in the water distribution system (Cartinella *et al.,* 2006; Cath *et al.,* 2010).

In recent years, a great deal of research has been directed for development of effective FO membranes, in particular aimed for lowering the membrane support structural parameters (S), increasing water permeability (A) and for selecting the most effective and efficient draw solutes that reduce energy consumption for draw solution recovery (Zhao *et al.,* 2012; Cath *et al*., 2006; Klaysom *et al.,* 2013). These efforts have resulted in substantially improved FO membranes. To name a few, high performance thin film composite FO membrane (Yip *et al.,* 2010) and aquaporin-based biomimetic FO membrane (Li *et al.,* 2015).

Because of the success in developing high performance FO membrane and the emergence of FO based spin-off companies, recent focus has also expands toward assessing membrane performance through module-scale analyses (Deshmukh *et al.,* 2015). A convenient and consistent methodology to characterize FO membranes is of critical importance to advance this technology into a more mature phase, facilitating sharing, interpretation, and data comparison (Tiraferri *et al.,* 2013; Bui *et al.*, 2015; Sulastri *et al.*, 2016). To support further progression for FO process development, a larger scale optimization is required to accurately envisage the most important factors to be explored. Module-scale assessment offer additional insight because it incorporates draw dilution and feed concentration effects, two phenomena that often ignored in lab-scale assessments.

By taking into account the membrane properties, operational parameters and the occurrence of CPs, mass-transfer models were have been developed to estimate FO membrane performance (Klaysom *et al.,* 2013). Those models were found correlate well with experiments using coupon size membrane samples and have been applied further to simulate performance of numerous large-scale FO modules, in particular for module development purpose(Jung *et al.,* 2011; Gruber *et al.,* 2011; Lee *et al.*, 2014; Xu *et al.,* 2010; Attarde *et al.,* 2015). However, during those simulations both flow and concentration of solute of feed and draw solutions are often assumed homogeneous. This assumption has proven inaccurate because spatial distribution of flow occurs even in a simple and small filtration cells (Gruber *et al.,*

DOI: http://dx.doi.org/10.17509/ijost.v1i2
p- ISSN 2528-1410 e- ISSN 2527-8045

2011), l*et al*one the complexity of flows in a module. As a result, the simulation results most likely overestimate the real values.

In this study, we applied a mass-transfer model coupled with the mass conservation to simulate the performance of plate and frame modules. The mass-transfer model includes the effect of the external and internal concentration effect as well as reverse salt diffusion (Bui *et al*., 2015), while the mass conservation accommodated the concentration (of feed stream) and dilution (of draw stream) effect occurs substantially in a large module area. Different possible operational parameters were simulated: modes (active layer facing feed solution, ALFS; and active layer facing draw solution, ALDS), flow orientations (co-, counter- and cross-current), spacers and spacer properties, membrane and operational parameters.

2. METHODOLOGY

2.1. Mass-transport model

Water (Jw, L/m^{2}h , LMH) and salt fluxes (Js, gMH) in a module were calculated by numerically solving mass-transfer (**Equations 1-4**) developed by Bui *et al*. (Bui *et al*., 2015). Those models account for contributions of membrane resistance, ICP, ECPs and solute back-transport. They can be solved numerically to obtain Jw and Js data, as long as membrane characteristics and operational parameters are provided.

For active layer facing feed solution mode (ALFS) also known as FO-mode, the water (Jw) and salt flux (Js) are given as follow:

$$J_w^{ALFS} = A\left[\frac{\pi_{D,b}\exp\left(-J_w\left[\frac{1}{k_D}+\frac{S}{D_D}\right]\right)-\pi_{F,b}\exp\left[\frac{J_w}{k_F}\right]}{1+\frac{B}{J_w}\left(\exp\left[\frac{J_w}{k_F}\right]-\exp\left(-J_w\left[\frac{1}{k_D}+\frac{S}{D_D}\right]\right)\right)}\right] \quad (1)$$

$$J_s^{ALFS} = B\left[\frac{C_{D,b}\exp\left(-J_w\left[\frac{1}{k_D}+\frac{S}{D_D}\right]\right)-C_{F,b}\exp\left[\frac{J_w}{k_F}\right]}{1+\frac{B}{J_w}\left(\exp\left[\frac{J_w}{k_F}\right]-\exp\left(-J_w\left[\frac{1}{k_D}+\frac{S}{D_D}\right]\right)\right)}\right] \quad (2)$$

For active layer facing draw solution mode (ALDS) also known as PRO-mode, the Jw and Js are given as follow:

$$J_w^{ALDS} = A\left[\frac{\pi_{D,b}\exp\left(\frac{-J_w}{k_D}\right)-\pi_{F,b}\exp\left[J_w\left(\frac{1}{k_F}+\frac{S}{D_F}\right)\right]}{1+\frac{B}{J_w}\left(\exp\left[J_w\left(\frac{1}{k_F}+\frac{S}{D_F}\right)\right]-\exp\left(-\frac{J_w}{k_D}\right)\right)}\right] \quad (3)$$

$$J_s^{ALDS} = B\left[\frac{C_{D,b}\exp\left(\frac{-J_w}{k_D}\right)-C_{F,b}\exp\left[J_w\left(\frac{1}{k_F}+\frac{S}{D_F}\right)\right]}{1+\frac{B}{J_w}\left(\exp\left[J_w\left(\frac{1}{k_F}+\frac{S}{D_F}\right)\right]-\exp\left(-\frac{J_w}{k_D}\right)\right)}\right] \quad (4)$$

A, B and S are water permeability coefficient (LMH/bar), solute permeability coefficient (m/s) and structural parameter (μm), respectively. Because of the small impact of Js, its contribution in defining module performance is neglected. This study only considers Jw to judge the module performance.

The π (osmotic pressure, bar) and D (diffusion coefficient, m^2/s) are function of solute concentrations (C, molar). The values of π and D can be obtained using empirical **equations 5** and **6** (Phuntsho *et al.,* 2014), when using NaCl as the solute and under constant temperature of 25 C. The equations were derived using OLI Stream Analyser 3.2

$$\pi = 3.805\,C^2 + 42.527\,C + 0.434 \quad (5)$$

$$D = (-1.025\,x\,10^{-10})C + 1.518\,x\,10^{-9} \quad (6)$$

DOI: http://dx.doi.org/10.17509/ijost.v1i2
p- ISSN 2528-1410 e- ISSN 2527-8045

The mass transfer coefficient (k, m s^{-1}) can be calculated as

$$k = \frac{S_h D}{d_h} \quad (7)$$

$$d_h = \frac{4\,b\,h}{2(b+h)} \quad (8)$$

where b is flow channel width (m) and h flow channel height (m). The value of flow channel height is equal to spacer thickness.

The Sherwood number for laminar flow is defined as in **Equation 9.** It is worth noting that laminar flow regime was observed for entire ranges of applied parameters.

$$S_h = 1.85 \left(R_e S_c \frac{d_h}{L}\right)^{0.33} \quad (9)$$

$$R_e = \frac{\rho v d_h}{\eta} \quad (10)$$

$$S_c = \frac{v}{D} \quad (11)$$

$$v = \frac{\mu}{\rho} \quad (12)$$

where L is length of the channel (m), Re Reynold number (-), Sc Schmit number (-), v cross flow velocity (m/s), ρ solution density (kg/m^3), v kinematic viscosity (m/s^2) and μ viscosity (kg/s.m). The values of ρ and μ are function of solute concentration (**equations 13** and **14**). The empirical relations between ρ and μ and C and solute concentration are as follow (Phuntsho *et al.*, 2014):

$$\rho = -1.047\,C^2 + 39.462\,C + 997.37 \quad (13)$$

$$\mu = (0.012\,C^2 + 0.065\,C + 0.895) \times 10^{-3} \quad (14)$$

Because the thermodynamics properties are given as a function of solute concentration, it is possible to capture the effect of feed concentration and draw solute dilution as a result of water flux and reverse salt flux inside the module.

2.2 Numerical modeling of FO module

Because of the large area of a module element, the solute concentrations in the feed and draw solution change as a function of location in the module. Therefore, the draw solute and feed concentration cannot be assumed constant at a particular value. To solve this situation, area discretization was implemented (**Figure 1**) by splitting the area into smaller cells. The area of 1 m^2 (1 m x 1 m) of one sheet module was split area into a hundred of 0.01 m^2 cells (0.1 m x 0.1 m). Because of the small area of the cell, it was also assumed that the solute concentrations within those small cells are constant. All simulations in this study assume a static condition in a steady state operation without considering membrane fouling (dynamic condition) or build-up condition (transient).

DOI: http://dx.doi.org/10.17509/ijost.v1i2
p- ISSN 2528-1410 e- ISSN 2527-8045

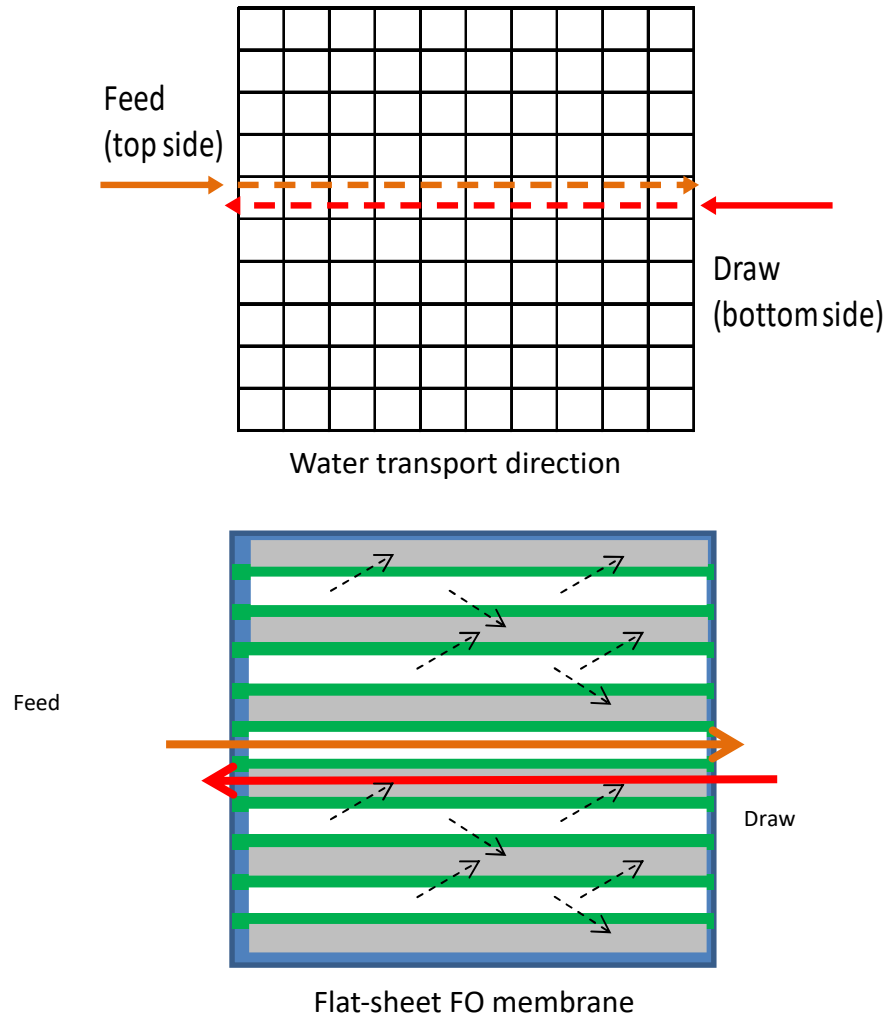

Figure 1. Schematic diagram of flows and area discretization of FO flat-sheet module in the counter-current flow orientation (top) and combined flow channel flow arrangement (bottom)

The concentration of solute over different cells affects each other because the feed and draw stream are coming into the cell either from the inlet or from other cell. To unravel the flow relations between cells, the flow is assumed to have only one dominant direction, either toward length or width, depending on cells locations and flow orientations. One direction flow means that the outlet of the first cell becomes the inlet of the second cell, and so . Fluid comes from one side and out through the opposite side of the cell, without spreading to another sides. The inlet of the first cells row is from the module inlet, the inlet of the next cell is from the outlet of the previous cell, while the outlet of the last cells is directly exit from module (see arrows in **Figure 1**). For the co-current flow, the calculation is simple because the flow of feed and draw solutions are in parallel. For the counter-current flow orientation, the calculations were performed through back-iteration. The mass-transport equations in **Equations 1-2** or **3-4** were solved simultaneously for each cells, in which the results of one cell become the input for solving the following cells.

DOI: http://dx.doi.org/10.17509/ijost.v1i2
p- ISSN 2528-1410 e- ISSN 2527-8045

2.3 SIMULATION PARAMETERS

The geometry of module was assumed to be 1x1 m stacked in 10 sheets per element with the default flow channel height of 1.14 mm (equal to the spacer thickness). The applied membrane properties and operational parameters are summarized in **Table 1**. To study the impact of commercial spacer, the spacer properties are summarized in **Table 2**

.

Tabel 1. Summary of simulation parameters. All simulations were run using parameters below, unless otherwise specified.

Parameters (unit)	value
Membrane parameters (HTI)	
Pure water permeability coefficient, A (L/m^{2}h bar)	1.02
Salt permeability coefficient, B (L/h)	0.464
Structural parameters, S (µm)	400
Module dimensions	
Flow channel height (m)	1.14 x 10^{-3}
Net length (m)	1 x 10^{-3}
Net width (m)	1 x 10^{-3}
Membrane sheet	10
Total module area (m^2)	10
Feed and draw solution	
Feed solute (gNaCl/L)	100
Feed solution flow rate (m^3/h)	1
Draw solute (gNaCl/L)	36
Draw solution flow rate (m^3/h)	0.34

Tabel 2. Summary of commercial feed/permeate spacer properties, adapted from (Schock and Miquel 1987).

	Parameters				
Commercial brand	Thickness (mm)	Filament thickness (mm)	Mesh length (mm)	Porosity	Specific surface (mm^{-1})
Toray PEC-1000	0.54	0.27	2.3	0.91	14.8
Naltex 1228	0.75	0.375	3	0.9	10.7
Desal RO	0.82	0.41	2.7	0.88	9.8
FilmTec FT30	0.77	0.385	2.8	0.89	10.4
Desal UF	1.51	0.755	3.1	0.81	5.3

DOI: http://dx.doi.org/10.17509/ijost.v1i2
p- ISSN 2528-1410 e- ISSN 2527-8045

The membrane sheet was arranged in combined flow mode in which a stream of feed is in contact with two membrane sheets (**Figure 1**). The same is applied to the stream of the draw. The simulation was only performed for the middle sheet in the 10-sheets module, because the two last channels under this module arrangement only in contact with one membrane sheet.

3. RESULTS AND DISCUSSION

3.1 Effect of flow orientation

Counter-current flow orientation shows slightly higher average flux in comparison to the co- and the cross-currents in ALFS-mode (**Figure 2** and **Table 3**), which is in line with other findings (Jung *et al.*, 2011; Phuntsho *et al.*, 2014; Gu *et al.*, 2011). Similar trend is also found for the ALDS-mode, with rather higher flux magnitudes. The rests two also exhibit a larger flux span (difference between maximum and minimum flux), which is less desirable because spatial flux distribution is known to promote membrane fouling (Lee *et al.,* 2014). The counter-current configuration was then applied for further simulation processes.

The large flux-span for the co- and cross current originates from the solute concentration of contacting feed and draw solution (notice arrows for feed and draw in **Figure 1**). For the co-current, the fresh draw (highest solute concentration) is in contact with the fresh feed (the lowest solute concentration) in the module entrance. This leads to the creation of the highest possible driving forces. Because of draw dilution and the feed concentration effects, the driving force is reduced toward the outlet of the module resulting in the lowest flux nearby the module exit. For the cross-current, the maximum and minimum osmotic driving forces occur at the first inlet of feed/draw corner (top left) and the last outlet of feed/draw corner (bottom right).

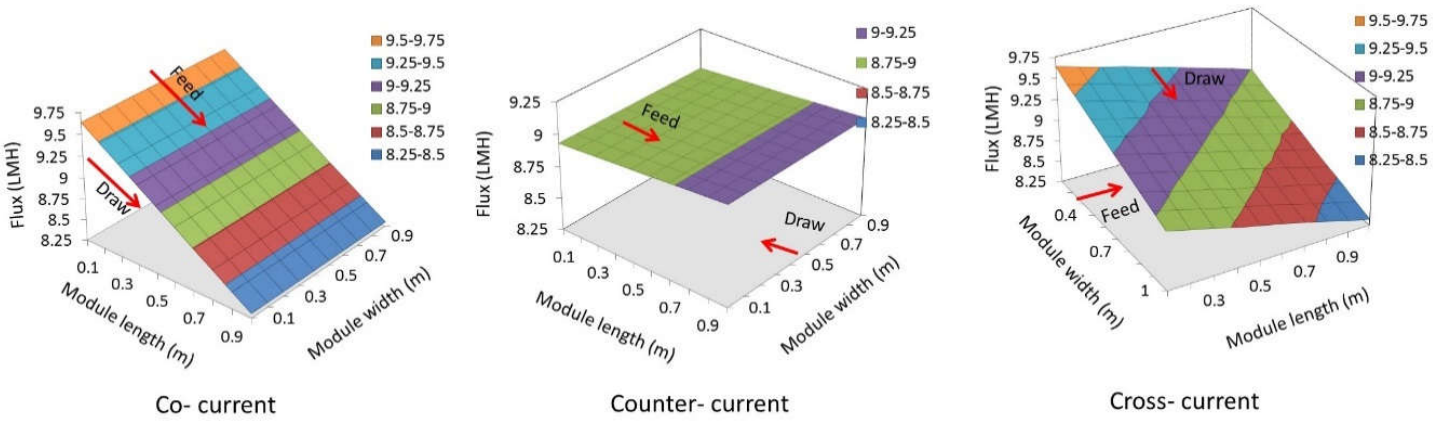

Figure 2. Effect of flow orientation on spatial flux distribution. The simulations were run using the following parameters: A=1.02 LMH/atm, B=0.464 m/s L/h, S=400 µm, FO-mode, Draw solution: 100 g/L NaCl, Feed solution: 36 g/L, draw flow rate: 1 m^3/h, feed flow rate: 0.34 m^3/h.

DOI: http://dx.doi.org/10.17509/ijost.v1i2
p- ISSN 2528-1410 e- ISSN 2527-8045

Tabel 3. Summary of module performances showing that counter-current flow orientation features the lowest spatial flux ranges and offers the highest average flux.

		Flux (LMH)			
Flow orientation	**Recovery**	**Average**	**Stdev**	**Range**	**%-range**
Co-current	28.87	8.97	0.43	1.336	14.89
Counter-current	28.98	8.98	0.03	0.095	1.06
Cross-current	28.86	8.97	0.3	1.312	14.63

Despite significant difference on the flux range (≈1% for counter-current and ≈15% for co- and cross-current), the average fluxes of different flow orientations are relatively close, unlike the one reported elsewhere (Phuntsho *et al.*, 2014). The deviation on the finding with the aforecited literature is due to the size of the simulated module dimension. This study only applies 10 m^2 membrane area, while Phuntsho *et al.* 2014 simulated up to 170 m^2 membrane area in a module. Their plot between module are and the flux also shows no significant different on flux at membrane area of 10 m^2. The smaller the module is the lesser the effect of flow orientation. For the large membrane area, the effects of concentration and dilution are more pronounced because the total mass of water transported across the membrane is larger.

3.2 Effect of membrane parameters

Among the three FO membrane parameters, A and S play major roles in determining transport performances (**Figure 3**). The results on the effects of B is not shown because it was insignificant. For simulating the effect of A, other parameters were maintained constant according to the values given in **Table 1**, and the same role was applied when simulating the effect of S. The simulations were run in ALDS-mode to achieve higher fluxes and clearer trend. Module scale simulation takes into account the effect of draw dilution and feed concentration, which are normally ignored in a lab-scale study because of the small size of the membrane coupon.

Significant flux improvements were only obvious when increasing the water permeability parameters up to 2 LMH/atm, by maintaining S at 400 µm. Up to that value, the average flux increases almost exponentially. Above that value, increasing A-value only slightly increases average fluxes. This phenomenon can be explained by depicting the contribution of ICP and ECPs. The latter is very small and does not clearly visible in **Figure 3** (top-right). However, the former seems to evolve as a function of the A-values. As the A-values increases, the contribution of ICP increases too, and its effect is more dominant when the A-values is high.

Average module flux increased as the S-parameters decreases (**Figure 3**, bottom). The trend is somewhat similar to the effect of A. Lowering the S-values from 500 to 250 µm, almost proportionally increases the average module flux. However, further reduction of S-values leads to exponential increase in fluxes. This trend can be explained by the contribution of ICP in the mass-transport. At high S-values (>250 µm), small changes of S only change the ICP slightly. However, as the S-values decreases further below 200 µm, the contribution of ICP shrinks, which leads to significant

DOI: http://dx.doi.org/10.17509/ijost.v1i2
p- ISSN 2528-1410 e- ISSN 2527-8045

increase in the effective mass-transport driving forces.

Overall findings on the impact of A and S parameters suggest that for FO membrane development, both parameters have to be developed simultaneously. As shown from the impact of A, increasing A-values only effective up to certain value because beyond that value the contribution of A on the mass transport is underwhelmed by the contribution of S in the ICP. From the effect of S data, for a given A-value of 1 LMH/atm, flux can significantly be improved when having S-values of less than 200 µm, under which the effect of ICP is suppressed. Increasing A-values only effective in improving flux when S-value is low.

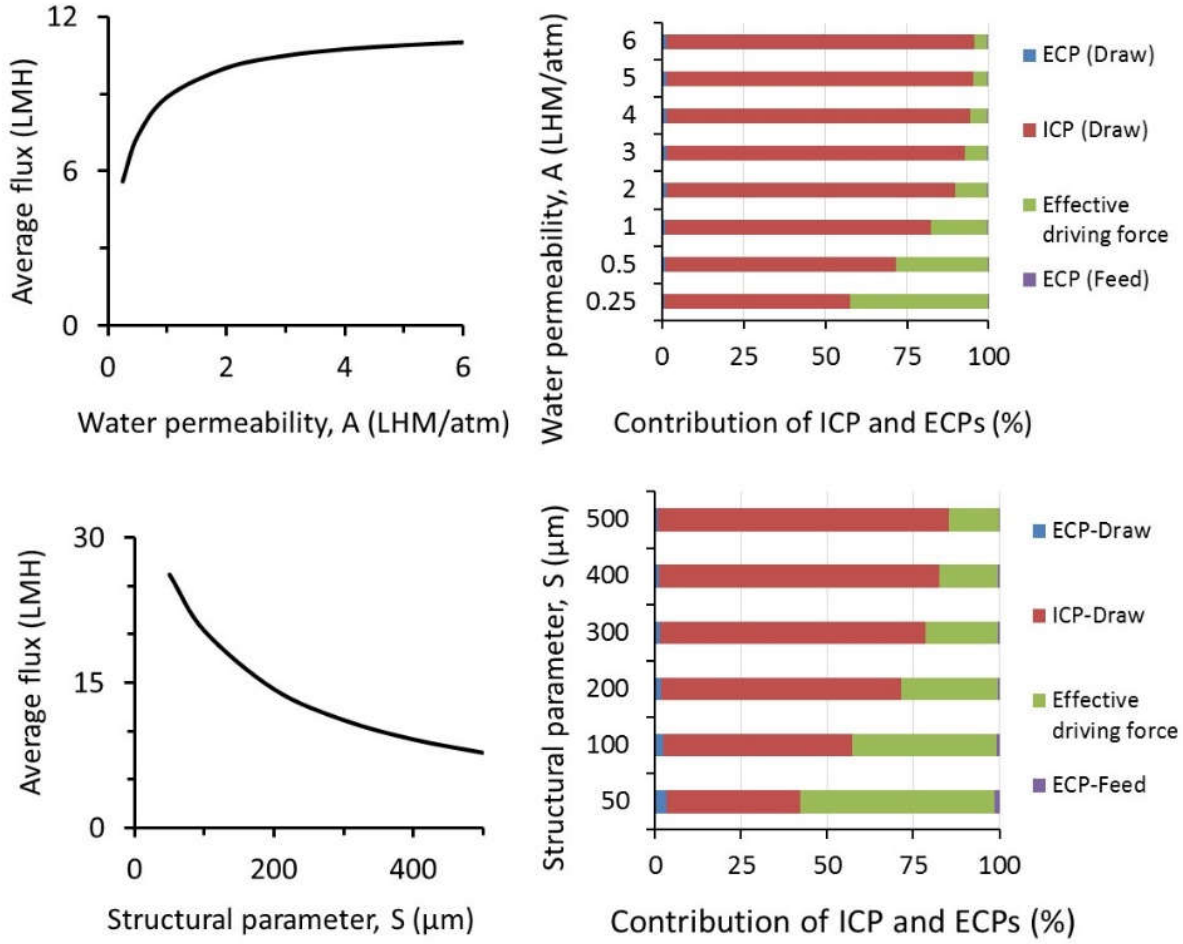

Figure 3. Effect of water permeability and structural parameters showing the trend (left) and explanation with respect to contribution of concentration polarizations.

3.3 Effect of spacer properties

The use of spacer in large scale membrane module is inevitable to support flow-channel integrity. Spacer-free flow channel only applicable in a small-scale flow channel in the lab-scale filtration cells. Nevertheless, spacer selection can be seen as a way to improve module performance (Schwinge *et al.*, 2004; Schock & Miquel, 1987). In addition for its use to maintain flow channel integrity, spacers has long been used as turbulence promoter. The presence of spacer in the flow channel can

DOI: http://dx.doi.org/10.17509/ijost.v1i2
p- ISSN 2528-1410 e- ISSN 2527-8045

help to break boundary layer, and thus help to reduce the impact of concentration polarization to lower membrane flux (Schwinge *et al.*, 2004).

The impact of spacer in enhancing average module flux is only moderate (up to 2% in comparison to the spacer-free flow channel). When comparing the effect of each spacer, the flow channel depth was also changed according to the spacer thickness. There is also no significant different between available commercial spacers, despite they feature different characteristics (range from 0.83 to 2.04% improvement). This finding deviates largely to the ones reported earlier (Schock & Miquel, 1987; Schwinge *et al.*, 2004), in which flux increase significantly in the presence of spacer. The lab-scale test of FO filtration in a different study also showed a flux increment of at least 10%, even at very low cross-flow velocities (data not shown).

The large deviations between our results and other references is because this study does not consider the role of spacer on the mass-transfer coefficient. Spacer changes the flow pattern and thus flow regime, which results in improving mass-transfer coefficient (Schock & Miquel, 1987). The impact of spacer on the mass-transfer coefficient will be included in the future study. In this study, spacer is only considered to change the cross-flow velocity and hydraulic diameter, in which spacer porosity plays the most crucial role in comparison to spacer surface area and spacer thickness. Increasing specific surface area slightly increases average flux, while reducing spacer thickness will reduce average flux. Spacer porosity directly correlates with linear velocity. Spacer with low porosity, occupy larger volume and thus lowering the cross-section area of the flow channel and lowering the hydraulic diameter. The less porous the spacer, the channel space occupied by the spacer is higher, thus promote an increase in cross-flow velocity that beneficial for improving mass-transfer coefficient.

3.4 Effect of operational parameters

Feed flow rate, draw and feed solute concentrations significantly affect average module flux (**Figure 5**). Increasing the feed flow rate increases mass-transfer coefficient and reduces the impact of ECPs. Increasing draw solute or decreasing feed solute concentrations directly corresponds to an increase in effective driving force of the osmotic process (**Equation 1-4**), and thus the water flux. As also shown in **Figure 4**, only minimum impact of spacer was observed by manipulating operational parameters.

Operational parameters are the last aspects that can be optimized to improve FO module performances, after a module has been build-up. Normally, their impacts are explored after optimizations of membrane (A, B, and S values) and module (spacer, module type, etc.) have been done. The freedom for operation is, however, also constrained by the process objectives. For instance, when the process is aimed for certain water recovery, all parameters have to be adjusted to meet that objective before additional engineering optimization can be done.

DOI: http://dx.doi.org/10.17509/ijost.v1i2
p- ISSN 2528-1410 e- ISSN 2527-8045

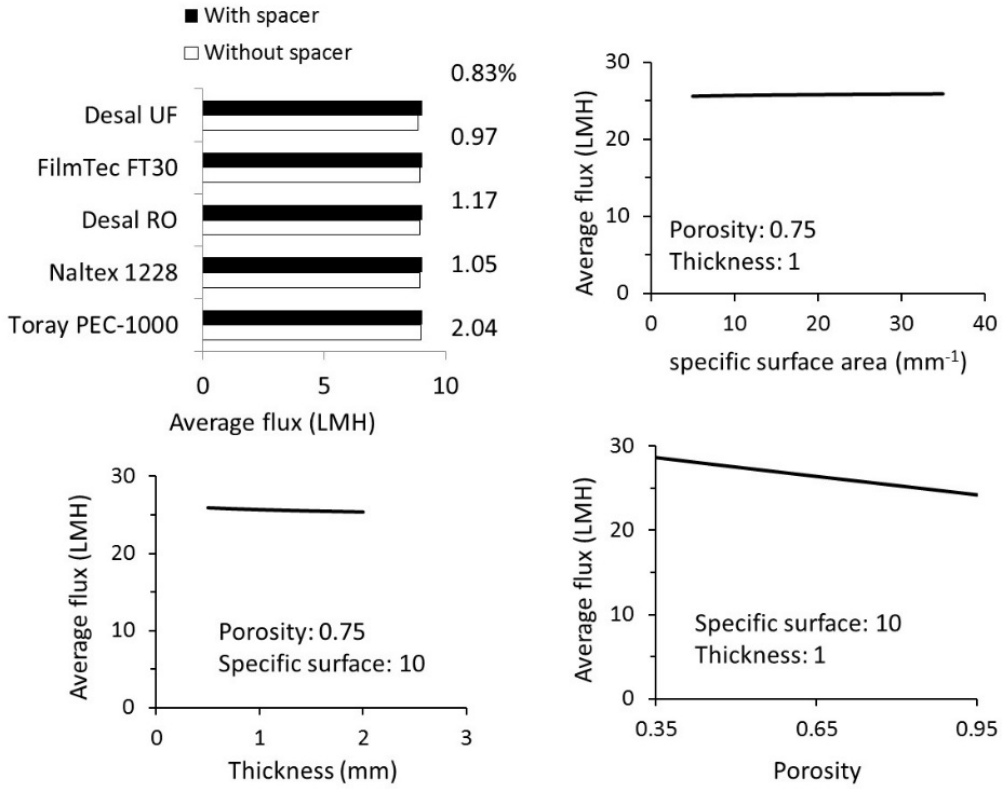

Figure 4. Effect of spacer types and spacer properties on average module flux in ALFS-mode.

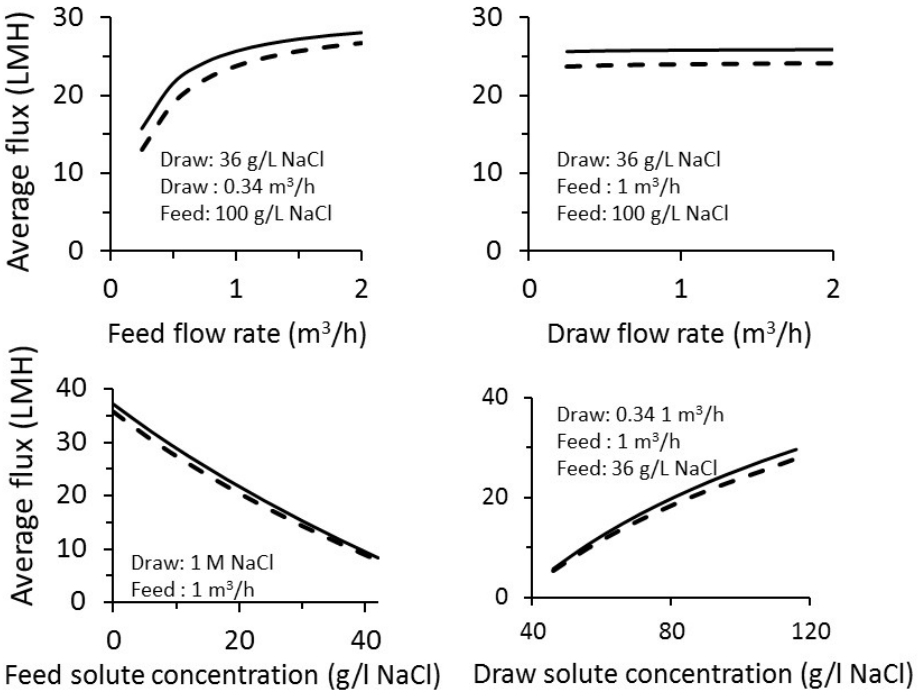

Figure 5. Effect of operational parameters. The full-lines show the performance of spacer filled channel, while the dashed-lines show the performance of spacer free channel. The simulations were performed using following parameters: A: 2 LMH/atm, S: 100 µm, ALFS-mode, counter-current flow orientation, spacer thickness 1 mm.

DOI: http://dx.doi.org/10.17509/ijost.v1i2
p- ISSN 2528-1410 e- ISSN 2527-8045

4. CONCLUSIONS

This study explore the impact of flow orientation, membrane properties, spacer properties and operational parameters on the performance of plate-and-frame FO module. Counter-current flow orientation offers higher flux and minimum spatial flux distribution. The later is very important, in particular, to distribute filtration load and thus minimizes its consequence on membrane fouling. Module performance can surely be improved by either lowering structural parameter or increasing water permeability. It is worth mentioning that both parameters are inter-dependent: increasing A-value will offer minimum impact without reducing S-value, and vice versa. Inclusion of spacer in the flow channel increases the flux, but its impact was poorly simulated. Moreover, module performance can be increased by increasing feed flow rate, lowering solute in the feed and increasing solute in the draw solution. Further study on different type of module (i.e., spiral wound) should be done to explore possible method to improve FO performance in a module-scale level. Application of more appropriate mass-transfer model is required to capture the effect of spacer accurately.

5. ACKNOWLEDGMENTS

Author acknowledge Universiti Teknologi PETRONAS for providing facilities for conducting the research activities.

6. AUTHOR'S NOTES

The author(s) declare(s) that there is no conflict of interest regarding the publication of this article. Authors confirmed that the data and the paper are free of plagiarism.

7. REFERENCES

Achilli, A., Cath, T. Y., Marchand, E. A., & Childress, A. E. (2009). The forward osmosis membrane bioreactor: a low fouling alternative to MBR processes. *Desalination*, *239*(1), 10-21.

Attarde, D., Jain, M., Chaudhary, K., & Gupta, S. K. (2015). Osmotically driven membrane processes by using a spiral wound module—Modeling, experimentation and numerical parameter estimation. *Desalination*, *361*, 81-94.

Bilad, M. R., Baten, M., Pollet, A., Courtin, C., Wouters, J., Verbiest, T., & Vankelecom, I. F. J. (2016). A novel In-situ Enzymatic Cleaning Method for Reducing Membrane Fouling in Membrane Bioreactors (MBRs). *Indonesian journal of science and technology*, *1*(1), 1-22.

Bui, N. N., Arena, J. T., & McCutcheon, J. R. (2015). Proper accounting of mass transfer resistances in forward osmosis: Improving the accuracy of model predictions of structural parameter. *Journal of membrane science*, *492*, 289-302.

Cartinella, J. L., Cath, T. Y., Flynn, M. T., Miller, G. C., Hunter, K. W., & Childress, A. E. (2006). Removal of natural steroid hormones from wastewater using membrane contactor processes. *Environmental science and technology*, *40*(23), 7381-7386.

Cath, T. Y., Childress, A. E., & Elimelech, M. (2006). Forward osmosis: principles, applications, and recent developments. *Journal of membrane science*, *281*(1), 70-87.

Cath, T. Y., Hancock, N. T., Lundin, C. D., Hoppe-Jones, C., & Drewes, J. E. (2010). A multi-barrier osmotic dilution process for simultaneous desalination and purification of impaired water. *Journal of membrane science*, *362*(1), 417-426.

Deshmukh, A., Yip, N. Y., Lin, S., & Elimelech, M. (2015). Desalination by forward osmosis: Identifying performance limiting parameters through module-scale modeling. *Journal*

of membrane science, *491*, 159-167.

Gruber, M. F., Johnson, C. J., Tang, C. Y., Jensen, M. H., Yde, L., & Hélix-Nielsen, C. (2011). Computational fluid dynamics simulations of flow and concentration polarization in forward osmosis membrane systems. *Journal of membrane science*, *379*(1), 488-495.

Gu, B., Kim, D. Y., Kim, J. H., & Yang, D. R. (2011). Mathematical model of flat sheet membrane modules for FO process: Plate-and-frame module and spiral-wound module. *Journal of membrane science*, *379*(1), 403-415.

Jung, D. H., Lee, J., Lee, Y. G., Park, M., Lee, S., Yang, D. R., & Kim, J. H. (2011). Simulation of forward osmosis membrane process: Effect of membrane orientation and flow direction of feed and draw solutions. *Desalination*, *277*(1), 83-91.

Klaysom, C., Cath, T. Y., Depuydt, T., & Vankelecom, I. F. (2013). Forward and pressure retarded osmosis: potential solutions for global challenges in energy and water supply. *Chemical society reviews*, *42*(16), 6959-6989.

Lee, J., Kim, B., & Hong, S. (2014). Fouling distribution in forward osmosis membrane process. *Journal of environmental sciences*, *26*(6), 1348-1354.

Lee, S., Boo, C., Elimelech, M., & Hong, S. (2010). Comparison of fouling behavior in forward osmosis (FO) and reverse osmosis (RO). *Journal of membrane science*, *365*(1), 34-39.

Li, X., Chou, S., Wang, R., Shi, L., Fang, W., Chaitra, G., ... & Fane, A. G. (2015). Nature gives the best solution for desalination: Aquaporin-based hollow fiber composite membrane with superior performance. *Journal of membrane science*, *494*, 68-77.

Mi, B., & Elimelech, M. (2010). Organic fouling of forward osmosis membranes: fouling reversibility and cleaning without chemical reagents. *Journal of membrane science*, *348*(1), 337-345.

Phuntsho, S., Hong, S., Elimelech, M., & Shon, H. K. (2014). Osmotic equilibrium in the forward osmosis process: modelling, experiments and implications for process performance. *Journal of membrane science*, *453*, 240-252.

Schock, G., & Miquel, A. (1987). Mass transfer and pressure loss in spiral wound modules. *Desalination*, *64*, 339-352.

Schwinge, J., Neal, P. R., Wiley, D. E., Fletcher, D. F., & Fane, A. G. (2004). Spiral wound modules and spacers: review and analysis. *Journal of membrane science*, *242*(1), 129-153.

Sulastri, A., & Rahmidar, L. (2016). Fabrication of Biomembrane from Banana Stem for Lead Removal. *Indonesian journal of science and technology*, *1*(1), 115-131.

Tiraferri, A., Yip, N. Y., Straub, A. P., Castrillon, S. R. V., & Elimelech, M. (2013). A method for the simultaneous determination of transport and structural parameters of forward osmosis membranes. *Journal of membrane science*, *444*, 523-538.

Xu, Y., Peng, X., Tang, C. Y., Fu, Q. S., & Nie, S. (2010). Effect of draw solution concentration and operating conditions on forward osmosis and pressure retarded osmosis performance in a spiral wound module. *Journal of membrane science*, *348*(1), 298-309.

Yip, N. Y., Tiraferri, A., Phillip, W. A., Schiffman, J. D., & Elimelech, M. (2010). High performance thin-film composite forward osmosis membrane. *Environmental science & technology*, *44*(10), 3812-3818.

Zhao, S., Zou, L., Tang, C. Y., & Mulcahy, D. (2012). Recent developments in forward osmosis: opportunities and challenges. *Journal of membrane science*, *396*, 1-21.

DOI: http://dx.doi.org/10.17509/ijost.v1i2
p- ISSN 2528-1410 e- ISSN 2527-8045